A Comparative Study of the Polar Version with the Subimage Version of Fast Factorized Backprojection in UWB SAR

T. K. Sjögren, V. T. Vu, M. I. Pettersson
Blekinge Institute of Technology
SE-371 79 Karlskrona, SWEDEN
email: thomas.sjogren@bth.se

Abstract: *This paper presents a comparative study of the polar and the subimage based variants of the time domain SAR algorithm Fast Factorized Backprojection. The difference between the two variants with regard to the phase error, which causes defocusing in the image, is investigated. The difference between the algorithms in interpolation between stages is also discussed. To investigate the sidelobes in azimuth, the paper gives simulation results for a low frequency UWB SAR system for both algorithms. How the algorithms differ with regard to amount of beams and length of beams is also discussed.*

1. Introduction

From the 1980s, interest for wide beam Ultra Wide Band (UWB) Synthetic Aperture Radar (SAR) increased due to its applications to high resolution and large area surveillance. The Fourier domain algorithms were unable to fully motion compensate the flight path in UWB SAR [1]. In response to this, time domain methods, which have the ability of UWB SAR imaging, were developed. The first time domain algorithm was Global Back Projection (GBP) [2]. The main advantages of GBP are the capability to produce high resolution SAR images and the much lower memory requirements for GBP compared to frequency domain algorithms, the disadvantage is that the algorithm consumes much more computation power compared to the traditional algorithms. From the 1990s, interest has grown within the area of SAR time domain processing and a couple of algorithms have been proposed which has the same benefit of motion compensation as GBP but at much lower computational cost [3-6]. First two stage algorithms [3-4] and later multi-stage algorithms [5-6] were developed giving further reduction in computation cost.

In [6], a multi stage time domain SAR algorithm called Fast Factorized Back Projection (FFBP) is introduced. One big advantage of FFBP compared to other multi-stage algorithms is that memory requirements can be traded against computation cost. FFBP is in [6] given in two variants, one polar and one subimage based variant. The two variants of FFBP have been introduced in the area of SAR [6-7], but to the knowledge of the authors only compared with each other within the area of Synthetic Aperture Sonar (SAS) [8-9].

2. Global Backprojection

GBP [2] is the backprojection of data from all pulses onto the Cartesian image grid. GBP is defined according to

$$h(x,\rho) = \int_{-\infty}^{\infty} g(x',R)R\,dx' \ , \tag{1}$$

where $R = \sqrt{(x'-x)^2 + \rho^2}$ is the range at aperture position x', $g(x',R)$ is the radar echo, x and ρ are azimuth and range image coordinates respectively. When applying a frequency ramp filter, GBP exactly solves the SAR imaging inversion [2] for a straight flight track and can easily be extended for SAR imaging under any arbitrary geometry of radar data acquisition. Therefore it has been proven a powerful algorithm for SAR imaging. Evaluating the

backprojection integral for an aperture of size N and an image of size N x N corresponds to a computational cost proportional to N^3. This is a much higher computational cost compared to the frequency domain algorithms, with a cost proportional to $N^2\log N$, and also compared to the recent faster time domain SAR imaging algorithms with a cost down to $N^2\log N$. Thus, when the SAR image is small, Global Backprojection [2] is a good choice due to the high SAR image quality obtained in combination with the low memory cost.
The strength in GBP's ability for high quality imaging for any data acquisition geometries is kept also with the faster variants of time domain imaging [3-6]. Algorithms [3-6] use the fact that the high Doppler frequency components of $g(x',R)$ changes slowly with x', and therefore limits the sampling in Doppler direction, according to the Nyquist criterion as derived in [3].

3. Fast Factorized Backprojection

In this paper we study the two variants of the algorithm introduced in [6], namely a polar version and a subimage version of FFBP. We name the variants Polar-FFBP (PFFBP) and SubImage-FFBP (SIFFBP). In general FFBP starts with pulse compressed radar echoes, and then uses a variable amount of beam forming stages before the final stage where the beams are backprojected onto the Cartesian image grid. The main differences of the two versions of FFBP are that the PFFBP samples the beams equidistantly in cosine of angle and that PFFBP does not apply factorization of the beams in range direction as illustrated in Figure 1. With regard to computational cost, both algorithms perform equal. The core of FFBP is the generation of new beams, based on old beams. This process is described according to [6] as the discrete version of

$$h(x,\rho)=\sum_{i=-\infty}^{+\infty}h(x_i,r_i,\vartheta_i)=\sum_{i=-\infty}^{+\infty}\sum_{j=-\frac{n-1}{2}}^{+\frac{n-1}{2}}h_{d/n}\left(x_0+(ni+j)\frac{d}{n},r'_j,\vartheta'_j\right)=\sum_{l=-\infty}^{+\infty}h_{d/n}\left(x_0+l\frac{d}{n},r'_l,\vartheta'_l\right) \qquad (2)$$

$$r'_j=\sqrt{(r_i\cos\vartheta_i+x_i+x_j')^2+(r_i\sin\vartheta_i)^2}\quad,\quad \vartheta_j=\arctan\left[r_i\sin\vartheta_i/(r_i\cos\vartheta_i+x_i-x'_j)\right]$$

Where r_i and ϑ_i is range and angle in the polar coordinate system with origin at the subaperture centre, and *i* index of subaperture and *j* index of sub-subaperture.

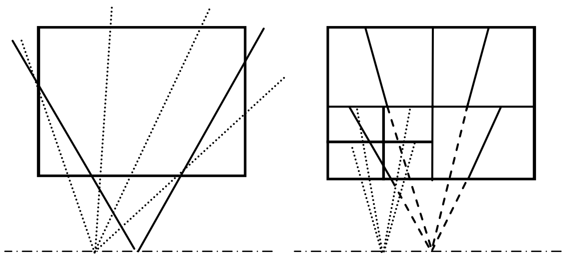

Figure 1. Beams in two stages of PFFBP and SIFFBP. Beams in stage 2 are dotted.

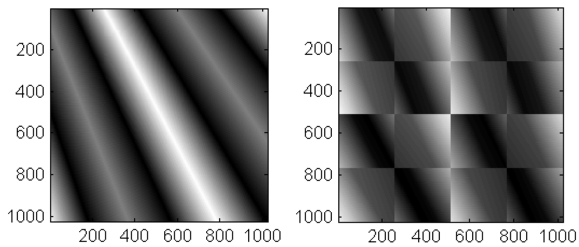

Figure 2. Phase error distribution in image through two stages of PFFBP and SIFFBP.

As seen in Figure 1, the amount of beams in SIFFBP is much higher, as the beam sampling density in angle increases with slantrange position of the subimage. However, the beam length is much shorter then for PFFBP which saves memory. It should also be noted that using nearest neighbour interpolation in angle, more then one parent beam always has to be considered. However, SIFFBP overcome the need for multiple beams by not strictly using nearest neighbour, instead the parent beam for the parent subimage is used directly. Thus, the interpolation between stages for SIFFBP is already inherent in the algorithm and is therefore very fast.

One other aspect of SIFFBP is its possibility of arbitrarily factorizing the subimages. This allows for subimages of different size over the image area, as well as a change in size of subimages with regard to the position of the subaperture. The earlier corresponds to areas further away on the image having larger subimages, thus reducing the computational cost of the SAR processing. The latter due to the fact that near range change for different subapertures. Another aspect of differences between the two variants is that in SIFFBP, the sampling in the Fourier domain is not equidistant in angle with more samples at high angles, while it is evenly distributed in angle for the polar version.

4. Error analysis

In [6] an error analysis is performed, where the maximum phase error due to nearest neighbour interpolation in angle at each stage of the algorithm is derived. According to [6], the maximum phase error for each stage is given by $2k\Delta R$, where ΔR is the range error

$$\Delta R = \sqrt{r^2 + t^2 - 2rt\cos(\vartheta + \phi)} - \sqrt{r^2 + t^2 - 2rt\cos\vartheta} \quad . \tag{3}$$

where r is range to the image pixel from the subaperture centre, t is distance from subaperture centre to the aperture position considered, ϑ is the angle to the image pixel position and ϕ the angle between the pixel and the beam centre. In [6] an upper bound for the absolute value of the range error is derived according to

$$|\Delta R| \le \frac{dD}{4r}, \tag{4}$$

where d is subaperture size and D is subimage size.

In Figure 2, the range error is shown for the two algorithms. The total range error is given in the SAR image using nearest neighbour interpolation. The images in Figure 2 were generated considering the error according to (3) for one subaperture through the two first stages of the algorithm. In the first stage 2 beams were used and in the second stage 4 beams corresponding to 4 subimages in first stage and 16 in the second. In the images the bright areas correspond to high range error, thus giving more defocusing in these areas. One observation is that the error for PFFBP is high in the centre of the image which is connected to the location in the middle of two beams in both stages. For SIFFBP, the error is higher in the corners of each subimage.

5. Simulation results

To evaluate the two variants, simulations of a point targets have been made using parameters according to the CARABAS-II system. The aperture size is 4096 positions and the aperture step size is 0.83 m. Near range of the image is 1414 m and the image size is 1024x1024 pixels. The images where formed using 4 stages, with a factorization step of 4 in each stage, corresponding to a maximum range error of 0.18m or $\lambda_{min}/17$ in each stage according to (4). For interpolation in range, upsampling was used. In angle, nearest neighbour was used. In the simulation, the settings are selected so that both algorithms have the same maximum range error throughout stages and the same computational cost.

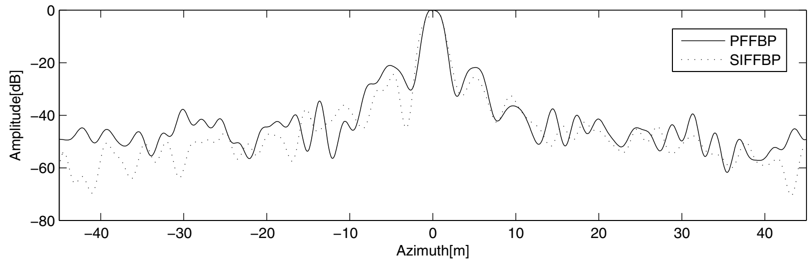

Figure 3. Azimuth sidelobes around simulated point target.

The ISLR obtained for SIFFBP is -13.6dB, while for PFFBP -14.7dB is obtained. As seen in Figure 3, the algorithms give similar peak levels of sidelobes, being able to suppress the sidelobes to approximately -20dB.

5. Conclusions and discussion

The paper has shown that in SAR imaging the two algorithms perform at a similar level with regard to image quality and that the obtained sidelobe level and ISLR can be good even without the use of angular interpolation kernels. The paper has also highlighted the differences of the two algorihms and shown the error distribution over the image scene. Another important issue is the possiblity of extending the algorithms for use with microwave SAR. In microwave SAR, autofocusing is often necessary for being able to correct the movements of the platform. When autofocusing, it is advantegous to have a strong scatterer in the scene. In the polar version of FFBP, the beams cover a larger extent of the image and therefore it is more likely there is at least one strong scatterer in the beam, allowing for more succesful autofocus for each beam.

References:

[1] Ulander L.M.H., Frölind P.-O., "Precision processing of CARABAS HF/VHF-band SAR data", *Proceedings of IGARSS 1999*, Hamburg, Germany, 28.6-2.7.1999, vol 1, pp47-49.

[2] Andersson L.E., "On Determination of a Function from Spherical Averages", *SIAM Journal of Applied Mathematics*, 1988, vol 19, pp214-341.

[3] Yegulalp A.F., "Fast backprojection algorithm for synthetic aperture radar", *IEEE Radar Conference 1999*, Waltham, USA, 20-22.4.1999, pp60-65.

[4] Seger O., Herberthson M., Hellsten H., "Real-time SAR processing of low frequency ultra wide band radar data", *Proceedings of EUSAR'1998*, 25-27.5.1998, Friedrichshafen, Germany, pp489-492.

[5] McCorkle J.W., Rofheart M., "An order $N^2\log(N)$ backprojector algorithm for focusing wide-angle wide-bandwidth arbitrary-motion synthetic aperture radar", *Proceedings of SPIE*, 1996, vol 2747, pp25-36.

[6] Ulander L.M.H., Hellsten H., Stenström G., "Synthetic-aperture radar processing using fast factorized back-projection", *IEEE Transactions on Aerospace and Electronic Systems*, 2003, vol 39, pp760-776.

[7] Frölind P.-O., Ulander L.M.H., "Evaluation of angular interpolation kernels in fast back-projection SAR processing", *IEE Proceedings in Radar, Sonar and Navigation*, 2006, vol 153, pp243-249.

[8] Callow H.J., Hansen R.E., Saebo T.O., "Effect of Approximations in Fast Factorized Backprojection in Synthetic Aperture Imaging of Spot Regions", *Oceans 2006*, Boston, USA, 18-21.9.2006, pp1-6.

[9] Shippey G., Banks S., Pihl J., "SAS Image reconstruction using Fast Polar Back Projection: comparisons with Fast Factored Back Projection and Fourier-domain imaging", *Oceans 2005* Europe, Brest, France, 20-23.06.2005, vol 1, pp96-101.